J Appl Physiol 130: 1604–1613, 2021.
First published March 25, 2021; doi:10.1152/japplphysiol.01062.2020

american physiological society | JOURNAL OF APPLIED PHYSIOLOGY

RESEARCH ARTICLE

Plasma gelsolin modulates the production and fate of IL-1β-containing microparticles following high-pressure exposure and decompression

Veena M. Bhopale,[1]* Deepa Ruhela,[1]* Kaighley D. Brett,[2] Nathan Z. Nugent,[2] Noelle K. Fraser,[2] Susan L. Levinson,[3] Mark J. DiNubile,[3] and Stephen R. Thom[1]

[1]*University of Maryland School of Medicine, Baltimore, Maryland;* [2]*Canadian Armed Forces Health Services, Ottawa, Canada; and* [3]*BioAegis Therapeutics, North Brunswick, New Jersey*

Abstract

Plasma gelsolin (pGSN) levels fall in association with diverse inflammatory conditions. We hypothesized that pGSN would decrease due to the stresses imposed by high pressure and subsequent decompression, and repletion would ameliorate injuries in a murine decompression sickness (DCS) model. Research subjects were found to exhibit a modest decrease in pGSN level while at high pressure and a profound decrease after decompression. Changes occurred concurrent with elevations of circulating microparticles (MPs) carrying interleukin (IL)-1β. Mice exhibited a comparable decrease in pGSN after decompression along with elevations of MPs carrying IL-1β. Infusion of recombinant human (rhu)-pGSN into mice before or after pressure exposure abrogated these changes and prevented capillary leak in brain and skeletal muscle. Human and murine MPs generated under high pressure exhibited surface filamentous actin (F-actin) to which pGSN binds, leading to particle lysis. In addition, human neutrophils exposed to high air pressure exhibit an increase in surface F-actin that is diminished by rhu-pGSN resulting in inhibition of MP production. Administration of rhu-pGSN may have benefit as prophylaxis or treatment for DCS.

NEW & NOTEWORTHY Inflammatory microparticles released in response to high pressure and decompression express surface filamentous actin. Infusion of recombinant human plasma gelsolin lyses these particles in decompressed mice and ameliorates particle-associated vascular damage. Human neutrophils also respond to high pressure with an increase in surface filamentous actin and microparticle production, and these events are inhibited by plasma gelsolin. Gelsolin infusion may have benefit as prophylaxis or treatment for decompression sickness.

decompression sickness; interleukin-1β; microparticles; neutrophils; oxidative stress

INTRODUCTION

Plasma gelsolin (pGSN) is an 84-kDa secreted isoform of a cytoplasmic actin-binding protein (1). It depolymerizes filamentous actin (F-actin), binds/sequesters an array of inflammatory mediators, and enhances macrophage phagocytosis and bactericidal actions (2–8). Blood levels fall in numerous acute and chronic inflammatory states. The magnitude of pGSN reduction parallels the extent of tissue damage, and depletion precedes and predicts adverse clinical outcomes (9–15). Protective effects with recombinant human (rhu)-pGSN administration have been reported in over 20 animal models of infection, injury, and inflammation (16). Its use as treatment for SARS-CoV-2-related pneumonia is in a phase II clinical trial (17). Because inflammatory responses play a role in the pathophysiology of decompression sickness (DCS), we hypothesized that a relationship may exist between pGSN and the stress imposed by high pressure and decompression (18–21).

Inert gases inhaled while breathing are taken up by tissues in proportion to the ambient pressure. When pressure is reduced, some of the gas released from tissues forms bubbles due to the presence of gas cavitation nuclei (22–24). The central place of bubbles as an inciting agent for DCS is widely accepted. However, because most decompression procedures generate asymptomatic blood-borne bubbles based on ultrasound studies, additional factors precipitating DCS are under investigation (25–27). High-pressure gases also trigger formation of small vesicles called microparticles (MPs) (28). The number of blood-borne MPs doubles in mice and humans exposed to high gas pressure and rises further after decompression (29–38). Murine studies indicate that MPs play a role in high-pressure gas pathophysiology and possibly gas bubble nucleation (37, 39–41). In a mouse model, MPs initiate a systemic inflammatory process related to neutrophil activation (37, 39–41). The pathway triggering MP formation also activates the nucleotide oligomerization domain (NOD)-like receptor, pyrin-containing 3 (NLRP3) inflammasome responsible for producing mature interleukin (IL)-1β (28, 42). Inflammasome assembly correlates with MP release, and MPs produced in response to high pressure contain high amounts of IL-1β,

* V. M. Bhopale and D. Ruhela contributed equally to this work.

Correspondence: S. R. Thom (sthom@som.umaryland.edu).

Submitted 11 December 2020 / Revised 16 February 2021 / Accepted 22 March 2021

which is the primary factor causing diffuse vascular damage in a murine DCS model (34, 43). When these MPs are purified and injected into naïve mice, they cause the same spectrum of injury as seen in decompressed mice (34, 37).

The goals of this study were to evaluate levels of pGSN in plasma from a previously reported human high-pressure exposure study (29) and to investigate pGSN in a murine DCS model. We hypothesized that the pGSN level would decrease with exposure to high pressure and decompression, and rhu-pGSN would abrogate vascular injuries in the murine model.

METHODS AND MATERIALS

Materials

Chemicals were purchased from Sigma Aldrich (St. Louis, MO), unless otherwise noted. Compressed gases were purchased from Air Products and Chemicals, Inc. (Allentown, PA). BioAegis Therapeutics (North Brunswick, NJ) provided rhu-pGSN. Antibodies and flow cytometry reagents are as follows: anti-actin (Sigma Aldrich, St. Louis, MO, Cat. No. A2066), anti-biotin (Sigma, Cat. No. B3640), anti-Ly6G eFluor450 (eBioscience, San Diego, CA, Cat. No. 48–5931-82), anti-mouse CD31 BV510 (Becton Dickinson/PharMingen, BD, San Jose, CA, Cat. No. 563089), annexin V-FITC (BD, Cat. No. 556419), anti-CD41 PerCP Cy5.5 (BioLegend, San Diego, CA, Cat. No. 133918), anti-CD45 Cy7-A (BioLegend, San Diego, CA, Cat. No. 103114), anti-gelsolin PE (Abcam, Cambridge, MA, Cat. No. ab109014), anti-IL-1β (Abcam, Cambridge, MA, Cat. No. ab9722), and NBD (N-[7-nitrobenz-2-oxa-1,3-thiazol-4-yl])-phalloidin (Life Technologies, Cat. No. N354). Verifications that anti-actin recognizes β-actin and anti-biotin recognizes biotinylated actin were shown by Western blot and mass spectroscopy in a prior publication (44). All antibodies for flow cytometry were specifically for this usage as documented by the manufacturers and used at the concentrations recommended, and positive staining was determined following the fluorescence-minus-one control test.

Animals

All aspects of this study were reviewed and approved by the Institutional Animal Care and Use Committee. C57BL/6J mice (*Mus musculus*) were purchased from Jackson Laboratories (Bar Harbor, ME). They were housed in the university animal facility with a 12/12-h light-dark cycle. Housing and all experiments were conducted at 22°C–24°C and 40%–70% humidity. Mice received water ad libitum and were fed Laboratory Rodent Diet 5001 (PMI Nutritional Inc., Brentwood, MO). Mice were left to breathe room air (control, ~100 kPa) or subjected to 2-h exposure to 790 kPa (absolute pressure) air in an ~10-L hyperbaric chamber with an air flow rate of 3 L/min to prevent CO_2 buildup, as described in previous publications (37, 41). In prior studies, the role of elevated N_2 partial pressure was shown to be the critical stressor causing pathological changes and not the mild elevations of O_2 that occur with 790 kPa air pressure (45). Where mentioned in the text, mice were injected with a sterile solution of rhu-pGSN (38.4 mg/mL) at a dose of 27 mg/kg intravenously or just the carrier buffer, immediately before or following decompression. At 2 h after decompression, animals were anesthetized and euthanized for blood and tissue collection as described previously (37, 41). Randomization of mice for experimentation was performed by first collecting all mice to be used in a day into a single plastic cage and then randomly selecting an individual mouse for use as the daily control or in an intervention group. Studies were done over a span of 4 mo with acclimatized mice purchased in groups of 6–12 at biweekly intervals and used according to a block design where individual blocks represented mice selected as control or pressure only and then with further experimentation including infusion of rhu-pGSN only or rhu-pGSN before or after pressure exposures. Data were scored and analyzed in a blinded manner such that the scorer did not know an animal's group assignment. All mice involved in this project were included in data analysis.

Human Subjects

All procedures were completed in accordance with the Declaration of Helsinki and approved by Ethical Committees of organizations involved with this investigation. Participants provided informed, written consent. Plasma samples analyzed in this project had been frozen and stored as part of a recently published study (29). A subgroup from this study included six male research subjects [34 ± 1.2 (SE) yr old] who in November 2018 were exposed to air at a pressure of 300 kPa, equivalent to 30 m of sea water (msw) for 35 min, and then staged decompression following Canadian Forces Standard Air Decompression Tables (DCIEM). Subjects remained sitting at rest with no exertion during the exposures and did not perform any specific tasks. Pressurization and decompression were conducted with filtered, pure air, and no breathing masks were used so as to prevent an elevation of CO_2. Data on MPs and IL-1β from these individuals were included in a previous publication (29). Blood samples were obtained 30 min before pressurization, after 25 min at pressure, and 2 h after decompression. Blood (~5 mL) was drawn into Cyto-Chex BCT test tubes that contain a proprietary preservative (Streck Inc., Omaha, NE), shipped to the senior author's laboratory, and processed as described previously (29). Plasma stored at −80°C after a 15,000 *g* centrifugation step preceding MP analysis was used for pGSN assays.

For ex vivo human cell studies, heparin-anticoagulated blood (4 mL) was obtained from healthy human volunteers and centrifuged through a two-layer preparation of Histopaque 1077 and 1119 (Sigma) at 400 *g* for 30 min to isolate neutrophils. The cells were washed in PBS, and a concentration of 9×10^5 neutrophils/mL of PBS + 1 mM $CaCl_2$, 1.5 mM $MgCl_2$, and 5.5 mM glucose were exposed at room temperature to either air at atmospheric pressure (~100 kPa) or air at a partial pressure of 790 kPa following published procedures (46).

Standard Procedures for MP Isolation

All reagents and solutions used for MP isolation and analysis were filtered with 0.1-μm filter (EMD Millipore, Billerica, MA). MPs were isolated and prepared for analysis by flow cytometry as previously described (37, 41). Briefly, blood was centrifuged for 5 min at 1,500 *g*. EDTA was added to the supernatant to achieve 12.5 mM to prevent MP aggregation and centrifuged at 15,000 *g* for 30 min. The supernatant was used for MP count and subtype analysis by flow cytometry as

described previously (37, 41), and samples were frozen at −80°C for later assays of IL-1β and pGSN.

MP Analysis

MPs were analyzed as described previously (37, 41). In brief, flow cytometry was performed with an eight-color, triple-laser MACSQuant Analyzer (Miltenyi Biotec Corp., Auburn, CA) using MACSQuantify software version 2.5 to analyze data. MACSQuant was calibrated every other day with calibration beads (Miltenyi Biotec Corp., Auburn, CA). Forward scatter and side scatter were set at logarithmic gain. Photomultiplier tube voltage and triggers were optimized to detect submicron particles. Microbeads of three different diameters, namely, 0.3 μm (Sigma, Inc., St. Louis, MO), 1.0 μm, and 3.0 μm (Spherotech, Inc., Lake Forest, IL), were used for initial settings and before each experiment as an internal control. Samples were suspended in annexin binding buffer solution [1:10 v/v in distilled water, (BD PharMingen, San Jose, CA)] and antibodies as listed in *Materials*. Binding by NBD-phalloidin was assessed to probe for the presence of F-actin. Examples of blood-borne particle analysis have been published previously (46). All reagents and solutions used for MP analysis were sterile and filtered (0.1-μm filter). MPs were defined as annexin V-positive particles with diameters of 0.3–1 μm. The concentration of MPs in sample tubes was determined by the MACSQuant Analyzer according to exact volume of solution from which MPs were analyzed.

Surface proteins on MPs from control and decompressed mice were biotinylated using sulfosuccinimidyl 2-(biotinamido)ethyl-1,3-dithiopropionate (NHS-SS-biotin) following methods similar to those described by others (47). The 15,000 *g* plasma supernatant was centrifuged at 100,000 *g* for 1 h, and MPs were resuspended in PBS without or with 100 mg/mL rhu-pGSN. After 30-min incubation at room temperature, ice-cold NHS-SS-biotin (0.9 mg/mL) was added, and samples were incubated on ice for 15 min. Biotinylation was quenched by addition of 100 mM glycine, and MPs were sedimented by centrifugation at 100,000 *g* for 1 h. The MP pellets were subjected to Western blotting or the biotinylated proteins were separated from MP lysates for analysis.

For Western blots, MPs were resuspended in 100 mM phosphate buffer with 2% sodium dodecyl sulfate (SDS), 10% glycerol, 5% β-mercaptoethanol, and 0.00125% bromophenol, followed by electrophoresis using a 4%–15% gradient polyacrylamide gel (SDS-PAGE), transfer to nitrocellulose paper, and then proteins probed for biotin, actin, and IL-1β. Alternatively, following ultracentrifugation, the MP pellets were resuspended in 100 μL of lysis buffer [20 mM Tris, 150 mM NaCl, 1% Nonidet P-40, 0.5% sodium deoxycholate, 1 mM EDTA, and 0.1% SDS (pH 7.5)] with protease inhibitors cocktail (Sigma) and incubated for 30 min on ice. MagVigen Streptavadin magnetic nanoparticles (Nvigen, Inc., Sunnyvale, CA) were then added and incubated for 12 h before the biotinylated proteins were separated for Western blotting using a magnet followed by washing and magnetic bead separation steps according to the manufacturer's recommended procedure.

Vascular Permeability Assay

Mice were injected with lysine-fixable tetramethylrhodamine-conjugated dextran (2×10^6 Da, Invitrogen, Carlsbad, CA), and endothelium-enriched tissue homogenates were prepared using colloidal silica following published methods (37, 41). Vascular permeability, quantified as perivascular dextran uptake in the experimental group, was normalized to a value obtained with a control mouse included in each experiment.

IL-1β Measurements

Human or mouse-specific ELISA kits (eBioscience, San Diego, CA) that detect pro and mature forms of IL-1β were used following the manufacturer's instructions. Measurements were made using plasma supernatant after blood was centrifuged at 15,000 *g* as described for flow cytometry studies and in MPs separated from plasma by centrifugation at 100,000 *g* for 60 min. The MPs pellets were placed in 0.3 mL of lysis buffer, protein content of the sample was measured, diluted to 5 mg/mL, and 20 μg of protein was used for analysis.

Gelsolin Assay

Human and mouse-specific commercial ELISA kits (LSBio, Inc. Seattle, WA) were used for measuring pGSN following the manufacturer's instructions. Serial dilutions in PBS were prepared using the supernatant after 15,000 *g* centrifugation of plasma and analyzed concurrent with a range of known pGSN standards.

Statistical Analysis

Results are expressed as means ± SE for three or more independent experiments. Data were compared by *t* test or analysis of variance (ANOVA) and the Newman–Keuls post hoc test using SigmaStat (Jandel Scientific, San Jose, CA). Data from human subjects were compared by repeated-measures analysis of variance (RM ANOVA) on ranks. For all studies, the level of statistical significance was defined as $P < 0.05$.

RESULTS

Human Studies—MPs, pGSN, and IL-1β

Blood samples from six research subjects were obtained before, during, and 2 h after exposure to 300 kPa air pressure in a dry hyperbaric chamber. Figure 1 demonstrates the relationships among MPs, pGSN, and plasma IL-1β. Exposure resulted in statistically significant elevations of MPs and IL-1β in plasma and a decrease in pGSN while at pressure with a further decrease of pGSN levels after decompression.

IL-1β secretion requires unconventional pathways, and a major route involves packaging into a vesicle to be liberated to the extracellular milieu (48). Therefore, intra-MP IL-1β concentrations were assessed as pg/million MPs among the six human subjects. Values were 24.5 ± 5.4 (SE) before pressure, 98.2 ± 17.5 at pressure, and 126.9 ± 20.8 after decompression ($P < 0.05$ among all 3 by RM ANOVA).

Murine Model—MPs, pGSN, and IL-1β

The impact in mice of exposure to 790 kPa air pressure for 2 h on the number of circulating MPs, pGSN, and IL-1β is shown in Fig. 2. Statistically significant changes were found

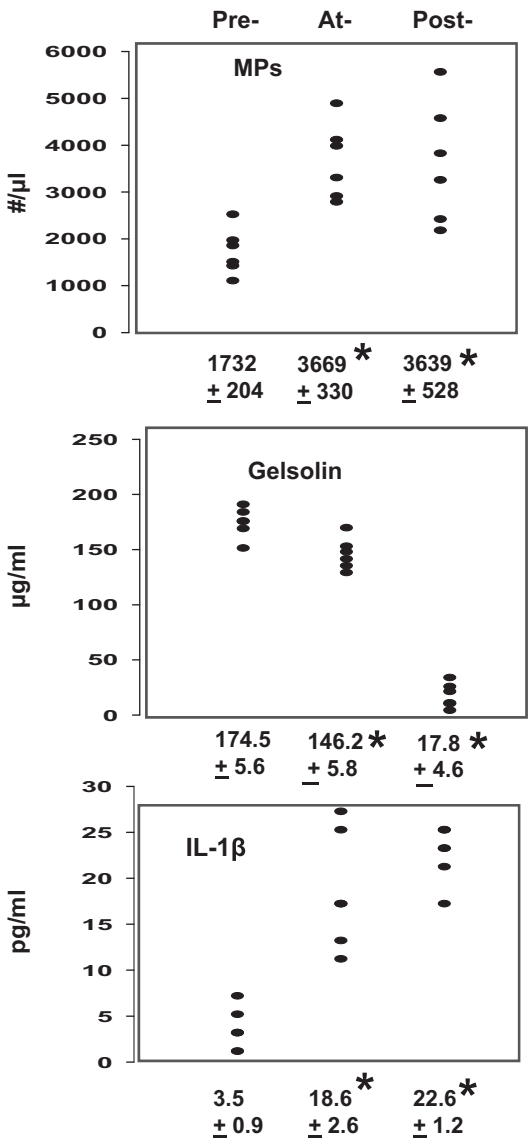

Figure 1. Changes in blood from human research subjects. The concentrations of pGSN and IL-1β were measured in plasma samples and blood-borne MPs were quantified preexposure, at-exposure, and postexposure to 300 kPa as described in METHODS. Individual data points are shown and below each plot are means ± SE, $n = 6$ for each sample, * indicates significantly different from preexposure, $P < 0.05$, RM ANOVA. IL-1β, interleukin-1β; MP, microparticles; RM, repeated-measures; pGSN, plasma gelsolin.

with elevations of MPs and plasma IL-1β concurrent with a decrease in pGSN. These changes were abrogated when mice were injected intravenously with rhu-pGSN immediately before pressurization or after decompression. Infusion of the carrier buffer used for rhu-pGSN injections had no significant effect on pressure responses, and infusions of rhu-pGSN into air-exposed control mice caused no statistically significant changes. The IL-1β concentrations expressed as pg/million MPs are shown in Table 1. Prophylactic rhu-pGSN administration did not prevent the increase in intraparticle IL-1β concentration, whereas treatment after decompression did abrogate the elevation (see 5th and last lines in Table 1).

Murine Model—Vascular Permeability

We next evaluated whether rhu-pGSN had an effect on tissue injury in the decompression model. Vascular permeability to rhodamine-labeled dextran was significantly elevated in skeletal muscle and brain at 2 h after decompression (Table 2). Vascular leakage was abrogated in mice that received rhu-pGSN before pressurization or immediately after decompression. Permeability was not significantly different from control when normal air-exposed mice were injected with rhu-pGSN.

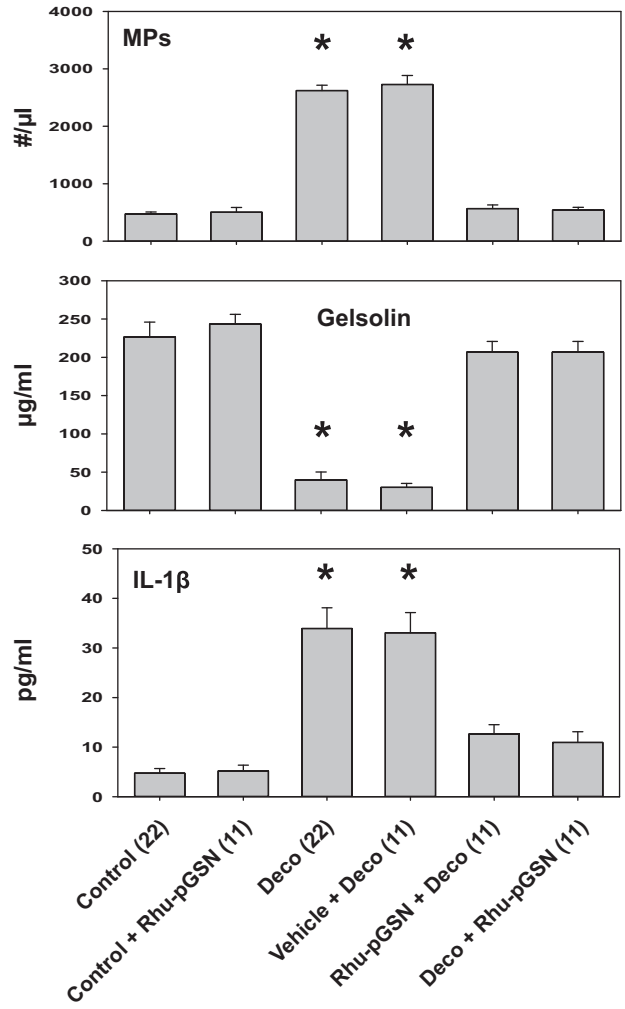

Figure 2. Changes in mice. Male mice were exposed to air at ambient pressure (control) or for 2 h to 790 kPa air, decompressed and euthanized 2 h later (Deco). Where indicated air-exposed control mice were injected intravenously with 27 mg/kg rhu-pGSN (Control + Rhu-pGSN) and euthanized 4 h later. Other mice were injected with rhu-pGSN prior to pressurization (Rhu-pGSN + Deco) or immediately after decompression (Deco + Rhu-pGSN), and others injected intravenously with the carrier buffer used to suspend rhu-pGSN (Vehicle + Deco), and these groups euthanized 2 h after decompression. The concentrations of mouse pGSN and IL-1β were measured in plasma samples by mouse-specific ELISAs and blood-borne MPs were quantified as described in METHODS. Data are expressed as means ± SE, the (n) for each sample is shown, *indicates significantly different from control, $P < 0.05$, ANOVA. IL-1β, interleukin-1β; MP, microparticles; rhu-pGSN, recombinant human-plasma gelsolin; pGSN, plasma gelsolin.

Table 1. *Murine IL-1β/million MPs*

Group	pg/million MPs
Control (19)	10.2 ± 1.2
Control + pGSN (18)	9.6 ± 1.3
Deco (1)	35.2 ± 6.1*
Vehicle + Deco (29)	33.8 ± 5.2*
pGSN + Deco (18)	47.9 ± 6.8*
Deco + pGSN (18)	13.9 ± 4.0

Data show the concentration of intra-MPs IL-1β (pg/million MPs) as means ± SE obtained from male mice manipulated as described in the caption for Fig. 2. The (*n*) for each group is shown, *indicates significantly different from control, $P < 0.05$, ANOVA. IL-1β, interleukin-1β; MP, microparticles; pGSN, plasma gelsolin.

MP Surface Protein Expression Patterns

MP subtypes were characterized based on expression of surface proteins. As in past studies, higher numbers of each subtype were found in decompressed mice (34–37). Values can be derived by multiplying total MP numbers by the percentage of each subtype shown in Table 3. However, we noted that strictly looking at percentage of each type offered insight into differences in possible cell sources for MPs. Table 3 demonstrates statistically significant differences from control in fractions of MPs expressing Ly6G (a neutrophil membrane protein) and those with a pattern consistent with endothelial cells [based on expression of CD31 (platelet-endothelial cell adhesion protein) but null for CD41 (a component of platelet-specific β_3 adhesion molecule)] from decompressed mice and decompressed mice injected with the carrier buffer. Among mice administered rhu-pGSN before or after decompression, the fraction expressing Ly6G was again significantly different from control, in contradistinction to the subtype expressing endothelial cell markers that was nearly at the control level. Hence, administration of rhu-pGSN prevented generation of endothelial-derived MPs in response to decompression. As expected, based on prior reports, when one adds up all the subtypes, the total exceeds 100%, likely indicating that surface proteins are shared among MPs due to collisions in the bloodstream (37).

Actin Presence on the MP Membrane

The loss of MPs in decompressed mice injected with rhu-pGSN could indicate that F-actin may be its target on the particle surface, given that one biochemical action of pGSN is to bind and then cleave F-actin (5, 11). To investigate this possibility, we used flow cytometry to evaluate whether fluorescently labeled phalloidin would bind to MPs. As shown in Table 3, the fraction of MPs that bound phalloidin increased eightfold in decompressed mice. Phalloidin binding by MPs was not significantly different from control among decompressed mice injected with rhu-pGSN.

Supporting evidence to assess whether actin was present on the MP surface was sought by selective surface-protein biotinylation using NHS-SS-biotin (see METHODS). Figure 3 is a representative Western blot of four replicates showing that the prominent 43-kDa biotinylated protein band is also recognized by anti-β-actin. In replicate experiments, the 43-kDa protein band of MPs from decompressed mice was 2.9 ± 0.3-fold denser than the band with control MPs ($n = 4$ replicates, $P < 0.05$, ANOVA). When incubated with 200 μg/mL rhu-pGSN (comparable with that of normal plasma, see Fig. 1), the band density of control MPs was reduced by 26.3 ± 4.3%, whereas with MPs from decompressed mice, the band density was decreased by 61.1 ± 3.2% ($P < 0.05$). No biotinylated protein bands were seen at 17 kDa or 31 kDa, where mature and pro-IL-1β, respectively, are located, nor were bands detected when Western blots were probed for IL-1β. IL-1β has been reported to be present inside but not adsorbed to the surface of MPs from decompressed mice (34). Therefore, NHS-SS-biotin labeled membrane surface proteins and did not gain access to internal MP proteins.

Biotinylated proteins were also separated from nonbiotinylated proteins for analysis. Figure 4 shows a representative Western blot using lysates from biotinylated MPs isolated from control and decompressed mice probed for biotin and β-actin. In four replicates, no IL-1β was detected. Furthermore, the results demonstrate that the majority of MP β-actin is present on the membrane surface and only scant amounts were detected in the biotin-negative MPs.

Ex Vivo Studies of Rhu-pGSN Incubations with Murine MPs

When MPs isolated from control and decompressed mice were suspended in buffer, particle numbers were stable over a 2-h ex vivo incubation (Fig. 5*A*). However, if rhu-pGSN was added to suspensions, the MPs from decompressed but not control mice were lysed. After each sample was fixed, fluorescent phalloidin and a fluorophore-labeled antibody that recognizes mouse and human pGSN were added to evaluate particle surface F-actin and pGSN binding. The Fig. 5*B* plot shows that the fraction binding phalloidin decreased for only the MPs from decompressed mice incubated with rhu-pGSN. Surface-bound pGSN values for the four groups were 11.5 ± 1.8% for control MPs, 12.1 ± 3.3% (NS) for control MPs where rhu-pGSN was added, 15.2 ± 3.6 (NS) for MPs from decompressed mice, and 26.6 ± 4.4 ($P < 0.05$, ANOVA) for MPs from decompressed mice where rhu-pGSN was added. These values did not change significantly over the course of the 2-h study.

Gelsolin can diminish phalloidin binding to F-actin due to F-actin cleavage and also because of displacement events (49, 50). We found that the kinetics of MP lysis and pGSN binding were not changed when experiments were done in the presence of equal concentrations of nonfluorescent and fluorescent phalloidin (data not shown), suggesting that the

Table 2. *Murine vascular leakage of 2 × 10^6 Da rhodamine-labeled dextran*

	Brain	Muscle
Control + pGSN (18)	1.1 ± 0.1	1.1 ± 0.1
Deco (29)	**4.8 ± 1.4***	**2.9 ± 1.5***
Vehicle + Deco (29)	**4.6 ± 0.9***	**2.3 ± 0.7***
pGSN + Deco (18)	1.3 ± 0.2	1.1 ± 0.2
Deco + pGSN (18)	1.4 ± 0.2	1.0 ± 0.2

Extravasation of dextran in brain and leg skeletal muscle was evaluated as described in METHODS in male mice manipulated as described in the caption for Fig. 2. Data are fold-difference in rhodamine-dextran/mg tissue protein (means + SE) vs. the values in control mice processed concurrently with each experimental group. Sample number is indicated as (*n*), *indicates significantly different from control, $P < 0.05$, ANOVA. pGSN, plasma gelsolin.

Table 3. *MPs subtypes in mice*

	%Ly6G	%CD14	%CD31	%CD41	%ECs	%Phall.
Control (19)	0.1 ± 0.1	44.3 ± 4.1	47.8 ± 5.7	29.1 ± 3.7	0.6 ± 0.1	2.3 ± 0.6
Control + pGSN (1)	1.0 ± 0.5	45.9 ± 5.1	36.1 ± 4.9	23.6 ± 4.4	0.8 ± 0.2	3.2 ± 0.7
Deco (1)	**11.1 ± 1.9***	51.2 ± 3.5	36.8 ± 3.4	18.0 ± 3.3	**2.3 ± 0.3***	**29.4 ± 3.3***
Vehicle + Deco (1)	**14.3 ± 2.5***	47.1 ± 3.3	49.4 ± 4.5	19.7 ± 3.4	**1.7 ± 0.2***	**24.5 ± 2.5***
pGSN + Deco (1)	**3.9 ± 0.9***	50.6 ± 3.2	38.9 ± 3.6	21.1 ± 3.5	0.4 ± 0.1	4.5 ± 1.0
Deco + pGSN (1)	**5.3 ± 0.8***	54.9 ± 6.8	40.2 ± 8.1	30.0 ± 5.7	0.5 ± 0.1	6.2 ± 2.0

Blood-borne MPs were quantified in male mice manipulated as described in the caption for Fig. 2 Flow cytometric measurements were made to quantify the number of all 0.3 to 1 μm diameter Annexin V-positive particles (data in Fig. 2) as well as the fraction of those expressing proteins specific to certain cells [Ly6G (mature neutrophils), CD14 (all leukocytes), CD31 (platelets and endothelium), CD41 (platelets), CD31+/ CD41-dim (endothelium, labeled ECs)] and also those that bound phalloidin (Phall). Data are expressed as means ± SE, n is shown for each sample; asterisk (*) and boldface indicates significantly different from control, $P < 0.05$, ANOVA. MP, microparticles; pGSN, plasma gelsolin.

reduction in fluorescent phalloidin bound to decompressed MPs was due to F-actin cleavage.

Ex Vivo Studies of Rhu-pGSN Incubations with Human Neutrophils

We examined effects of rhu-pGSN on human neutrophils because prior studies have shown that neutrophils play a major role in MP generation and vascular damage in the DCS model (21, 34, 37, 43). We reported previously that when human cells are incubated at high gas pressure, MP production is maximal in 30 min with no further production whether cells remain at pressure or they are decompressed (28). Human neutrophils (1.5×10^5 in 200 μL of buffer) generated 1,885 ± 139 (SE, n = 10) MPs/μL over 30 min when exposed to 790 kPa air pressure. If cells were incubated at 790 kPa in the presence of 200 μg/mL rhu-pGSN, significantly fewer MPs, 657 ± 93/μL (n = 10, $P < 0.05$), were produced. Cell suspensions incubated in air at ambient pressure had 493 ± 71 MPs/μL at the start of incubations and 538 ± 52 MPs/μL at the end (not significantly different), and numbers were unchanged in the presence of rhu-pGSN.

We then investigated neutrophil suspensions that were first incubated in air at ambient pressure or at 790 kPa for 30 min and rhu-pGSN added to each after pressure. Time 0 in Fig. 6 indicates addition of 200 μg/mL rhu-pGSN. At 30-min intervals, the cells and MPs in samples were fixed, separated by centrifugation, and analyzed by flow cytometry. Although rhu-pGSN had no effect on neutrophil number or viability (data not shown), it did impact surface-staining pattern of decompressed cells. The first plot demonstrates the fraction of neutrophils that stained with fluorescent phalloidin. Control cells exhibited relatively low phalloidin binding and no significant change with time. Phalloidin binding on cells first subjected to pressure was significantly different from control but decreased with time in the presence of rhu-pGSN. The second plot shows neutrophil staining with gelsolin antibody. Again, control cells exhibited relatively low staining and no change with time. However, cells that had

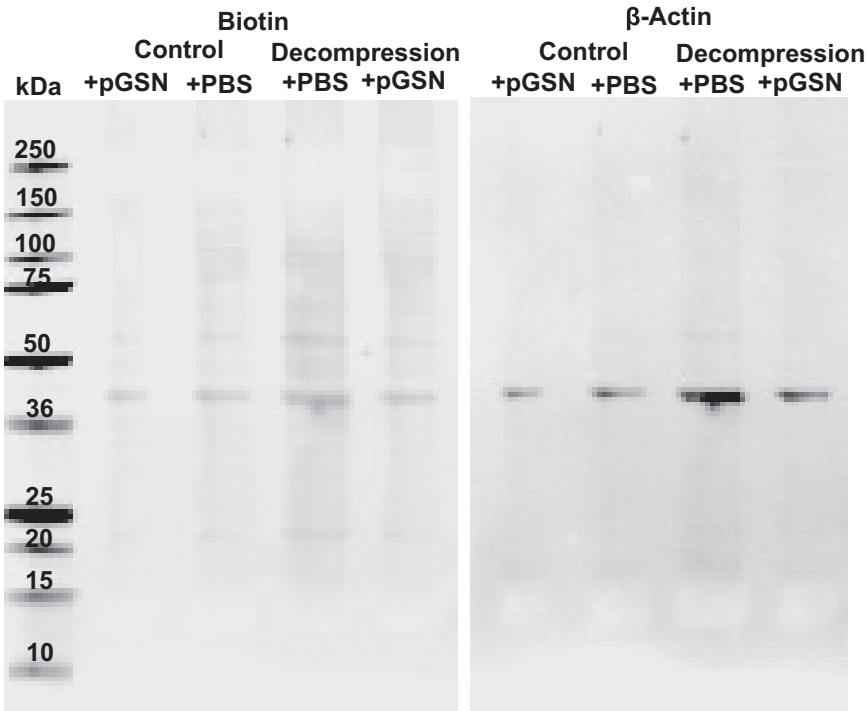

Figure 3. Biotinylation of MPs proteins. MPs from control and decompressed male mice were isolated, incubated with 200 mg/mL rhu-pGSN (shown as + pGSN) or just PBS, and then biotinylated as described in METHODS. MPs were then lysed in SDS buffer and protein from 45,500 MPs loaded into each lane for SDS-PAGE. Western blots probed for biotin and for β-actin are shown. Probing for IL-1β did not demonstrate bands (not shown). Molecular weight standards (in kDa) are shown at *left*. IL-1β, interleukin-1β; MP, microparticles; rhu-pGSN, recombinant human-plasma gelsolin; pGSN, plasma gelsolin.

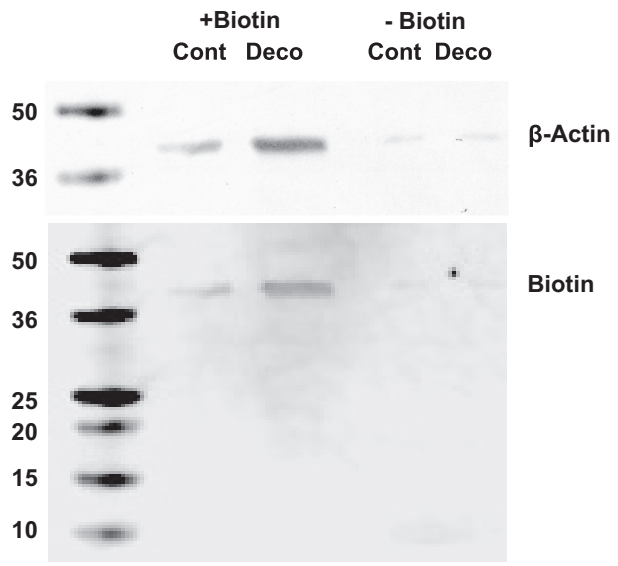

Figure 4. Biotinylated vs. nonbiotinylated MPs separation: MPs from control and decompressed male mice were isolated, biotinylated, and then lysed. Samples were incubated with magnetic streptavidin beads as described in METHODS and passed through a magnet to separate biotinylated (shown as +Biotin) from nonbiotinylated proteins (shown as −Biotin). Protein from 165,000 MPs was loaded into each lane for SDS-PAGE. Western blots probed for β-actin and biotin are shown. Probing for IL-1β did not demonstrate bands (not shown). Molecular weight standards (in kDa) are shown at *left*. IL-1β, interleukin-1β; MP, microparticles.

been exposed to high pressure had significantly more gelsolin antibody staining, and values decreased over 2 h in parallel with the drop in phalloidin binding.

The next three rows in Fig. 6 show data pertaining to the MPs present in the suspensions. Addition of rhu-pGSN to control preparations did not alter the number of MPs, phalloidin binding, or gelsolin antibody binding. In pressure-exposed suspensions where rhu-pGSN was added, the number of MPs and fraction with high phalloidin binding decreased significantly with time, whereas the fraction staining with gelsolin antibody increased.

DISCUSSION

Exposure to high pressure decreases pGSN in blood of humans and mice concurrently with elevations of MPs and IL-1β (Figs. 1 and 2). In mice, MPs containing high concentrations of IL-1β are responsible for causing diffuse capillary leak (34, 43). Surface proteins expressed on MPs in decompressed mice exhibited significantly more CD31+/CD41-dim, consistent with endothelial activation/damage, and Ly6G, indicative of a neutrophil origin (Table 3). Administration of rhu-pGSN to mice before or after pressure/decompression prevented elevations in the total number of MPs, the IL-1β concentration in plasma, the MPs subset from endothelium, and capillary leakage (Fig. 2, Table 2). When rhu-pGSN was administered prophylactically, intra-MP IL-1β concentration was elevated after decompression, whereas rhu-pGSN treatment after decompression resulted in an intra-MP IL-1β concentration that was not significantly different from control (Table 1). We believe these differences can be explained by the data evaluating the impact of rhu-pGSN on MPs and neutrophils ex vivo.

One biochemical action of pGSN is to bind and then cleave F-actin, a process that is thought to abrogate intravascular injuries and organ damage (5, 11). Others have shown a complementary relationship between circulating F-actin and pGSN levels, the presence of pGSN-actin complexes in plasma, and depletion of circulating pGSN with local sequestration at injured sites (9, 11, 12, 51). Figures 3 and 4 show that actin is present on the MP membrane surface, especially those from decompressed mice, and phalloidin binding (Table 3, Fig. 5) indicates the presence of F-actin. Similarly, MPs produced by high gas pressure-stimulated human neutrophils ex vivo also exhibit high phalloidin binding (Fig. 6). When rhu-pGSN is added to murine or human MP suspensions, it binds preferentially to pressure-generated MPs, and MPs lyse as the fraction binding phalloidin drops. Therefore, the data suggest pGSN is binding to F-actin and cleavage renders the MPs sensitive to osmotic lysis.

We interpret the inverse relationship between circulating pGSN and MPs in humans and mice with pressure exposure (Figs. 1 and 2) as arising because pGSN binds to the increasing number of MPs. Moreover, Table 3 demonstrates that the fraction of MPs binding phalloidin in decompressed mice injected with rhu-pGSN was not significantly different from control. This observation suggests that MPs lysis is selective and rhu-pGSN did not destroy MPs exhibiting low phalloidin

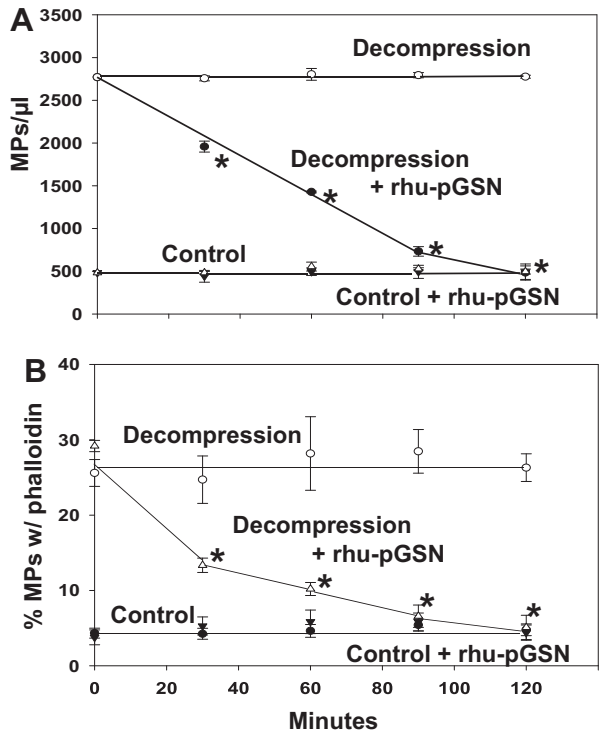

Figure 5. Effect of rhu-pGSN on MPs from control and decompressed mice. Blood was obtained from control or decompressed male mice and centrifuged as described in METHODS. MPs suspensions were divided and where shown at time 0, 200 μg/mL rhu-pGSN was added. At 30-min intervals, samples were fixed. The number of remaining MPs and the percentage of particles that bound fluorescent phalloidin were quantified. Data are expressed as means ± SE, $n = 5$ for each sample, *indicates significantly different from the value at time 0, $P < 0.05$, RM-ANOVA. MP, microparticles; rhu-pGSN, recombinant human-plasma gelsolin; RM, repeated-measures; pGSN, plasma gelsolin.

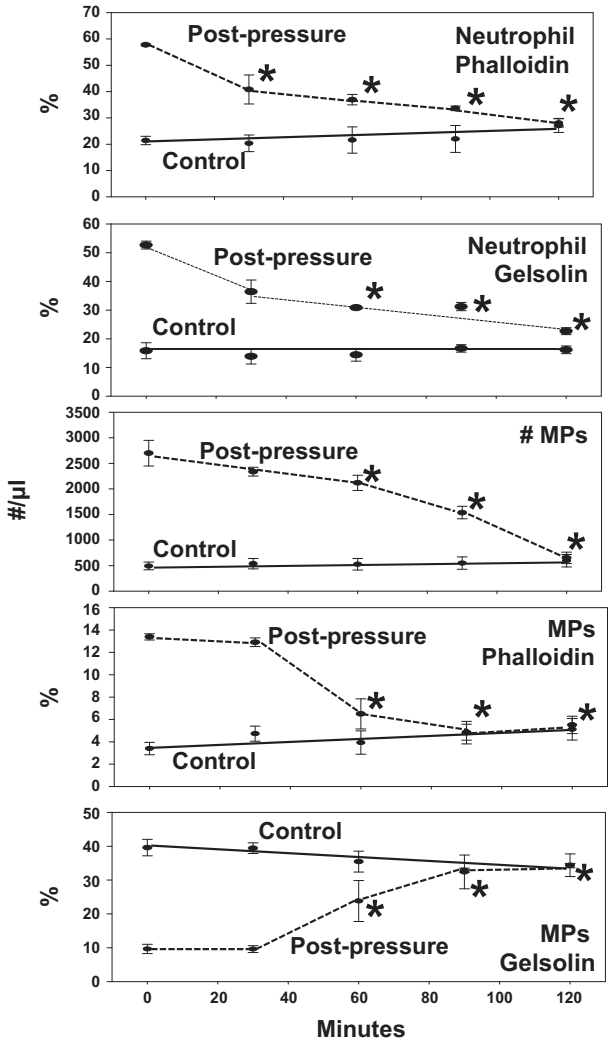

Figure 6. Effect of rhu-pGSN on human neutrophils and MPs. Neutrophils were isolated, incubated for 30 min in ambient air or at 790 kPa, and decompressed. At time 0 time, rhu-pGSN (200 µg/mL) was added and at 30-min intervals portions of samples were fixed and processed as described in METHODS to quantify MPs, binding of anti-gelsolin antibody and fluorescent phalloidin. Data are expressed as means ± SE, $n = 4$ for each sample, *indicates significantly different from the value at time 0, $P < 0.05$, RM-ANOVA. MP, microparticles; rhu-pGSN, recombinant human-plasma gelsolin; RM, repeated-measures; pGSN, plasma gelsolin.

binding. The same relationship is seen with ex vivo murine MPs in Fig. 5 and human MPs in Fig. 6. Rhu-pGSN lysed the phalloidin-positive MPs, leaving the same number of MPs in the preparations after the 2-h incubations as were present in the control samples. However, phalloidin binding is not a quantitative index of susceptibility for lysis by rhu-pGSN. Approximately 20% of postpressure murine MPs in Fig. 5 and 14% in Fig. 6 exhibited phalloidin binding at time 0, and the fraction dropped to ~4% over the 2-h studies. In this same period, the total number of MPs dropped by ~80% (from 2,600–2,800/µL to ~500–520/µL). This difference may occur because F-actin binding on some MPs is below the threshold of detection by flow cytometry or because of additional pGSN ligands such as anionic phospholipids on MPs.

Actin has been detected on the membrane surface of platelets, neutrophils, monocytes, lymphocytes, endothelial cells, and sympathoadrenal/catecholaminergic cells (52–57). A recent study found that macrophage MP generation requires extracellular F-actin, which appears to influence caspase-1 activation at filopodia (58). We found that ~80% of human neutrophils exposed to high gas pressure ex vivo exhibited phalloidin binding versus just 20% of control cells (Fig. 6). High-pressure inert gases stimulate neutrophils by triggering oxidative stress (28), and it now appears that F-actin expression on the cell surface is associated with this process. It seems reasonable that extracellular F-actin is transferred to the newly generated MPs budding from the cell surface in response to pressure, explaining why pressure-generated MPs exhibit higher phalloidin binding and why rhu-pGSN selectively impacts decompressed mouse MPs versus the MPs of control mice (Figs. 2 and 5) and pressure-generated human MPs (Fig. 6).

We found that gelsolin antibody will bind to control mouse and human MPs. With regard to the human neutrophil studies (Fig. 6), MPs are not generated during incubations at ambient pressure, so the MPs present in control samples were carried through from plasma. The control MPs appear to have only scant F-actin, as they exhibited relatively low phalloidin binding (~3.5%), but pGSN appears to be present on ~40% of the MPs based on antibody binding. This discrepancy could occur if there is an alternative mechanism for pGSN binding other than F-actin. One possibility may relate to the high affinity pGSN has for binding to fibronectin. Others have shown that pGSN cell attachment can be mediated via soluble fibronectin, which will attach to cell membranes via integrins and glycoproteins (59, 60).

Figure 6 also shows that rhu-pGSN cleaves F-actin on the postdecompression neutrophil surface, as demonstrated by the drop in phalloidin binding. Binding by the pGSN antibody decreased in parallel, suggesting that as F-actin is cleaved, pGSN can no longer bind to the neutrophil membrane. In addition, we found that inclusion of rhu-pGSN with human neutrophils while exposed to high pressure inhibits MPs production by ~65% (1,885 ± 139 MPs/µL vs. 657 ± 93/µL). Thus, surface F-actin may be needed for MP generation in response to gas pressure. This reflects a separate action in addition to direct MPs lysis, and the effect could be the basis for differences noted in intra-MPs IL-1β concentration between mice infused with rhu-pGSN prophylactically versus injection after decompression (see Table 1). Administration after decompression destroys virtually all pressure-induced MPs, including the ones carrying high IL-1β, whereas prophylactic rhu-pGSN administration impedes but does not entirely prevent MPs generation.

Results from this study highlight the role of MPs as a cytokine carrier. IL-1β is cleared from the plasma within 2 h after injection of rhu-pGSN in decompressed mice (Fig. 2). Simply lysing MPs would not immediately diminish the plasma concentration of IL-1β, but lysis abrogates capillary leak mediated by IL-1β (34, 43). Hence, MPs appear to have an important role targeting IL-1β to endothelium. This is an area that remains poorly understood and worthy of future research. Our results suggest that supplementation with rhu-pGSN can prevent or reverse DCS by reducing inflammatory

MPs. This represents a new action for rhu-GSN that may have relevance to a broad number of inflammatory injuries.

Another obvious issue in need of further investigation is the time course for MP elevations and greater detail on mechanism for formation. As shown in this study, exposures of humans (~35 min) and mice (2 h) differed yet achieved similar MP elevations. Prior work has described differences in MP production rates for mice, humans, and murine and human neutrophils based on pressure and exposure gas(es) (28–41).

ACKNOWLEDGMENT

The authors would especially like to acknowledge the assistance of Dr. Thomas P. Stossel who offered valuable insight into plasma gelsolin (pGSN) as this investigation was progressing.

GRANTS

This work was supported by the US Office of Naval Research Grant N00014-20-1-2641, by the Canadian Forces Surgeon General Health Research Program, and an unrestricted grant from the National Foundation of Emergency Medicine.

DISCLOSURES

S.L. Levinson and M.J. DiNubile are employed by and own stock in BioAegis Therapeutics, which is developing recombinant human plasma gelsolin for clinical use. Other authors declare that they have no conflicts of interest.

AUTHOR CONTRIBUTIONS

S.R.T. conceived and designed research; V.M.B., D.R., K.D.B., N.Z.N., N.K.F., and S.R.T. performed experiments; S.R.T. analyzed data; S.R.T. interpreted results of experiments; S.R.T. prepared figures; S.R.T. drafted manuscript; V.M.B., D.R., K.D.B., N.Z.N., N.K.F., S.L.L., M.J.D., and S.R.T. edited and revised manuscript; V.M.B., D.R., K.D.B., N.Z.N., N.K.F., S.L.L., M.J.D., and S.R.T. approved final version of manuscript.

REFERENCES

1. **Kwiatkowski DJ**, **Stossel TP**, **Orkin SH**, **Mole JE**, **Colten HR**, **Yin HL.** Plasma and cytoplasmic gelsolins are encoded by a single gene and contain a duplicated actin-binding domain. *Nature* 323: 455–458, 1986. doi:10.1038/323455a0.
2. **Bucki R**, **Byfield FJ**, **Kulakowska A**, **McCormick ME**, **Drozdowski W**, **Namiot Z**, **Hartung T**, **Janmey PA.** Extracellular gelsolin binds lipoteichoic acid and modulates cellular response to proinflammatory bacterial wall components. *J Immunol* 181: 4936–4944, 2008. doi:10.4049/jimmunol.181.7.4936.
3. **Bucki R**, **Georges PC**, **Espinassous Q**, **Funaki M**, **Pastore JJ**, **Chaby R**, **Janmey PA.** Inactivation of endotoxin by human plasma gelsolin. *Biochemistry* 44: 9590–9597, 2005. doi:10.1021/bi0503504.
4. **Bucki R**, **Kulakowska A**, **Byfield FJ**, **Zendzian-Piotrowska M**, **Baranowski M**, **Marzec M**, **Winer JP**, **Ciccarelli NJ**, **Gorski J**, **Drozdowski W**, **Bittman R**, **Janmey PA.** Plasma gelsolin modulates cellular response to sphingosine 1-phosphate. *Am J Physiol Cell Physiol* 299: C1516–C1523, 2010. doi:10.1152/ajpcell.00051.2010.
5. **Ordija CM**, **Chiou TT**, **Yang Z**, **Deloid GM**, **de Oliveira Valdo M**, **Wang Z**, **Bedugnis A**, **Noah TL**, **Jones S**, **Koziel H**, **Kobzik L.** Free actin impairs macrophage bacterial defenses via scavenger receptor MARCO interaction with reversal by plasma gelsolin. *Am J Physiol Lung Cell Mol Physiol* 312: L1018–L1028, 2017. doi:10.1152/ajplung.00067.2017.
6. **Osborn TM**, **Dahlgren C**, **Hartwig JH**, **Stossel TP.** Modifications of cellular responses to lysophosphatidic acid and platelet-activating factor by plasma gelsolin. *Am J Physiol Cell Physiol* 292: C1323–C1330, 2007. doi:10.1152/ajpcell.00510.2006.
7. **Vartanian AA.** Gelsolin and plasminogen activator inhibitor-1 are Ap3A-binding proteins. *Ital J Biochem* 52: 9–16, 2003.
8. **Yang Z**, **Chiou TT**, **Stossel TP**, **Kobzik L.** Plasma gelsolin improves lung host defense against pneumonia by enhancing macrophage NOS3 function. *Am J Physiol Lung Cell Mol Physiol* 309: L11–L16, 2015. doi:10.1152/ajplung.00094.2015.
9. **Khatri N**, **Sagar A**, **Peddada N**, **Choudhary V**, **Chopra BS**, **Garg V**, **Garg R**, **Ashish.** Plasma gelsolin levels decrease in diabetic state and increase upon treatment with F-actin depolymerizing versions of gelsolin. *J Diab Res* 2014: 152075, 2014. doi:10.1155/2014/152075.
10. **Lee PS**, **Patel SR**, **Christiani DC**, **Bajwa E**, **Stossel TP**, **Waxman AB.** Plasma gelsolin depletion and circulating actin in sepsis: a pilot study. *PLoS One* 3: e3712, 2008. doi:10.1371/journal.pone.0003712.
11. **Lee PS**, **Sampath K**, **Karumanchi SA**, **Tamez H**, **Bhan I**, **Isakova T**, **Gutierrez OM**, **Wolf M**, **Chang Y**, **Stossel TP**, **Thadhani R.** Plasma gelsolin and circulating actin correlate with hemodialysis mortality. *J Am Soc Nephrol* 20: 1140–1148, 2009. doi:10.1681/ASN.2008091008.
12. **Lu C-H**, **Lin S-T**, **Chou H-C**, **Lee Y-R**, **Chan H-L.** Proteomic analysis of retinopathy-related plasma biomarkers in diabetic patients. *Arch Biochem Biophys* 529: 146–156, 2013. doi:10.1016/j.abb.2012.11.004.
13. **Osborn TM**, **Verdrengh M**, **Stossel TP**, **Tarkowski A**, **Bokarewa M.** Decreased levels of the gelsolin plasma isoform in patients with rheumatoid arthritis. *Arthritis Res Ther* 10: R117, 2008. doi:10.1186/ar2520.
14. **Overmyer KA**, **Shishkova E**, **Miller IJ**, **Balnis J**, **Bernstein MN**, **Peters-Clarke TM**, **Meyer JG**, **Quan Q**, **Muehlbauer LK**, **Trujillo EA**, **He Y**, **Chopra A**, **Chieng HC**, **ITiwari A**, **Judson MA**, **Paulson B**, **Brademan DR**, **Zhu Y**, **Serrano LR**, **Linke V**, **Drake LA**, **Adam AP**, **Schwartz BS**, **Singer HA**, **Swanson S**, **Mosher DF**, **Stewart RD**, **Coon JJ**, **Jaitovich A.** Large-scale multi-omic analysis of COVID-19 severity. *medRxiv*, 2020. doi:10.1101/2020.07.17.20156513.
15. **Peddada N**, **Sagar A**, **Ashish Garg R.** Plasma gelsolin: a general prognostic marker of health. *Med Hypotheses* 778: 203–210, 2012. doi:10.1016/j.mehy.2011.10.024.
16. **Piktel E**, **Levental I**, **Durnaś B**, **Janmey P**, **Bucki R.** Plasma gelsolin: indicator of inflammation and its potential as a diagnostic tool and therapeutic target. *Int J Mol Sci* 19: 2516, 2018. doi:10.3390/ijms19092516.
17. **Global Newswire**. *BioAegis Therapeutics Initiates Phase 2 Clinical Trial of Its Inflammation Regulator, Gelsolin, for COVID-19 Treatment*. https://www.globenewswire.com/news-release/2020/08/05/2073785/0/en/BioAegis-Therapeutics-Initiates-Phase-2-Clinical-Trial-of-Its-Inflammation-Regulator-Gelsolin-for-COVID-19-Treatment.html. [5 August 2020]
18. **Bigley NJ**, **Perymon H**, **Bowman GC**, **Hull BE**, **Stills HF**, **Henderson RA.** Inflammatory cytokines and cell adhesion molecules in a rat model of decompression sickness. *J Interferon Cytokine Res* 28: 55–63, 2008. doi:10.1089/jir.2007.0084.
19. **Little T**, **Butler BD.** Pharmacological intervention to the inflammatory response from decompression sickness in rats. *Aviat Space Environ Med* 79: 87–93, 2008. doi:10.3357/asem.2118.2008.
20. **Philp RB.** A review of blood changes associated with compression-decompression: relationship to decompression sickness. *Undersea Biomed Res* 1: 117–150, 1974.
21. **Thom SR**, **Bennett M**, **Banham ND**, **Chin W**, **Blake DF**, **Rosen A**, **Pollock NW**, **Madden D**, **Barak O**, **Marroni A**, **Balestra C**, **Germonpre P**, **Pieri M**, **Cialoni D**, **Le PN**, **Logue C**, **Lambert D**, **Hardy KR**, **Sward D**, **Yang M**, **Bhopale VB**, **Dujic Z.** Association of microparticles and neutrophil activation with decompression sickness. *J Appl Physiol (1985)* 119: 427–434, 2015. doi:10.1152/japplphysiol.00380.2015.
22. **Fox FE**, **Herzfeld KF.** Gas bubbles with organic skins as cavitation nuclei. *J Acoust Soc Am* 26: 984–989, 1954. doi:10.1121/1.1907466.
23. **Yount DE.** On the elastic properties of the interfaces that stabilize gas cavitation nuclei. *J Colloid Interface Sci* 193: 50–59, 1997. doi:10.1006/jcis.1997.5048.
24. **Yount DE**, **Kunkle TD**, **D'Arrigo JS**, **Ingle FW**, **Yeung CM**, **Beckman EL.** Stabilization of gas cavitation nuclei by surface-active compounds. *Aviat Space Environ Med* 48: 185–189, 1977.
25. **Eftedal OS**, **Lydersen S**, **Brubakk AO.** The relationship between venous gas bubbles and adverse effects of decompression after air dives. *Undersea and Hyperbaric Med* 34: 99–105, 2007.

26. **Ljubkovic M**, **Dujic Z**, **Mollerlokken A**, **Bakovic S**, **Obad A**, **Breskovic T**, **Brubakk AO.** Venous and arterial bubbles at rest after no-decompression air dives. *Med Sci Sports Exerc* 43: 990–995, 2011. doi:10.1249/MSS.0b013e31820618d3.
27. **Ljubkovic M**, **Marinovic J**, **Obad A**, **Breskovic T**, **Gaustad SE**, **Dujic Z.** High incidence of venous and arterial gas emboli at rest after trimix diving without protocol violations. *J Appl Physiol (1985)* 109: 1670–1674, 2010. doi:10.1152/japplphysiol.01369.2009.
28. **Thom SR**, **Bhopale VM**, **Yang M.** Neutrophils generate microparticles during exposure to inert gases due to cytoskeletal oxidative stress. *J Biol Chem* 289: 18831–18845, 2014. doi:10.1074/jbc.M113.543702.
29. **Brett KD**, **Nugent NZ**, **Fraser NK**, **Bhopale VM**, **Yang M**, **Thom SR.** Microparticle and interleukin-1B production with human simulated compressed air diving. *Sci Rep* 9: 13320, 2019. doi:10.1038/s41598-41019-49924-41591.
30. **Madden D**, **Thom SR**, **Milovanova TN**, **Yang M**, **Bhopale VM**, **Ljubkovic M**, **Dujic Z.** Exercise before SCUBA diving ameliorates decompression-induced neutrophil activation. *Med Sci Sports Exerc* 46: 1928–1935, 2014. doi:10.1249/MSS.0000000000000319.
31. **Madden D**, **Thom SR**, **Yang M**, **Bhopale VM**, **Milovanova TN**, **Ljubkovic M**, **Dujic Z.** High intensity cycling before SCUBA diving reduces post-decompression microparticle production and neutrophil activation. *Eur J Appl Physiol* 114: 1955–1961, 2014. doi:10.1007/s00421-014-2925-7.
32. **Madden LA**, **Chrismas BC**, **Mellor D**, **Vince RV**, **Midgley AW**, **McNaughton LR**, **Atkin SL**, **Laden G.** Endothelial function and stress response after simulated dives to 18 msw breathing air or oxygen. *Aviat Space Environ Med* 81: 41–45, 2010. doi:10.3357/asem.2610.2010.
33. **Pontier JM**, **Gempp E**, **Ignatescu M.** Blood platelet-derived microparticles release and bubble formation after an open-sea air dive. *Appl Physiol Nutr Metab* 37: 888–892, 2012. doi:10.1139/h2012-067.
34. **Thom SR**, **Bhopale VM**, **Yu K**, **Yang M.** Provocative decompression causes diffuse vascular injury in mice mediated by microparticles containing interleukin-1beta. *J Appl Physiol (1985)* 125: 1339–1348, 2018. doi:10.1152/japplphysiol.00620.2018.
35. **Thom SR**, **Milovanova TN**, **Bogush M**, **Bhopale VM**, **Yang M**, **Bushmann K**, **Pollock NW**, **Ljubkovic M**, **Denoble P**, **Dujic Z.** Microparticle production, neutrophil activation, and intravascular bubbles following open-water SCUBA diving. *J Appl Physiol (1985)* 112: 1268–1278, 2012. doi:10.1152/japplphysiol.01305.2011.
36. **Thom SR**, **Milovanova TN**, **Bogush M**, **Yang M**, **Bhopale VM**, **Pollock NW**, **Ljubkovic M**, **Denoble P**, **Madden D**, **Lozo M**, **Dujic Z.** Bubbles, microparticles, and neutrophil activation: changes with exercise level and breathing gas during open-water SCUBA diving. *J Appl Physiol (1985)* 114: 1396–1405, 2013. doi:10.1152/japplphysiol.00106.2013.
37. **Thom SR**, **Yang M**, **Bhopale VM**, **Huang S**, **Milovanova TN.** Microparticles initiate decompression-induced neutrophil activation and subsequent vascular injuries. *J Appl Physiol (1985)* 110: 340–351, 2011. doi:10.1152/japplphysiol.00811.2010.
38. **Vince RV**, **McNaughton LR**, **Taylor L**, **Midgley AW**, **Laden G**, **Madden LA.** Release of VCAM-1 associated endothelial microparticles following simulated SCUBA dives. *Eur J Appl Physiol* 105: 507–513, 2009. doi:10.1007/s00421-008-0927-z.
39. **Thom SR**, **Yang M**, **Bhopale VM**, **Milovanova TN**, **Bogush M**, **Buerk DG.** Intra-microparticle nitrogen dioxide is a bubble nucleation site leading to decompression-induced neutrophil activation and vascular injury. *J Appl Physiol (1985)* 114: 550–558, 2013. doi:10.1152/japplphysiol.01386.2012.
40. **Yang M**, **Kosterin P**, **Salzberg BM**, **Milovanova TN**, **Bhopale VM**, **Thom SR.** Microparticles generated by decompression stress cause central nervous system injury manifested as neurohypophiseal terminal action potential broadening. *J Appl Physiol (1985)* 115: 1481–1486, 2013. doi:10.1152/japplphysiol.00745.2013.
41. **Yang M**, **Milovanova TN**, **Bogush M**, **Uzun G**, **Bhopale VM**, **Thom SR.** Microparticle enlargement and altered surface proteins after air decompression are associated with inflammatory vascular injuries. *J Appl Physiol (1985)* 112: 204–211, 2012. doi:10.1152/japplphysiol.00953.2011.
42. **Thom SR**, **Bhopale VM**, **Yu K**, **Huang W**, **Kane MA**, **Margolis DJ.** Neutrophil microparticle production and inflammasome activation by hyperglycemia due to cytoskeletal instability. *J Biol Chem* 292: 18312–18324, 2017. doi:10.1074/jbc.M117.802629.
43. **Thom SR**, **Bhopale VM**, **Yang M.** Microparticle-induced vascular injury in mice following decompression is inhibited by hyperbaric oxygen: effects on microparticles and interleukin-1beta. *J Appl Physiol (1985)* 126: 1006–1014, 2019. doi:10.1152/japplphysiol.01109.2018.
44. **Thom SR**, **Bhopale VM**, **Mancini DJ**, **Milovanova TN.** Actin S-nitrosylation inhibits neutrophil beta2 integrin function. *J Biol Chem* 283: 10822–10834, 2008. doi:10.1074/jbc.M709200200.
45. **Yang M**, **Bhopale VM**, **Thom SR.** Separating the roles of nitrogen and oxygen in high pressure-induced blood-borne microparticle elevations, neutrophil activation, and vascular injury in mice. *J Appl Physiol (1985)* 119: 219–222, 2015. doi:10.1152/japplphysiol.00384.2015.
46. **Bhullar J**, **Bhopale VM**, **Yang M**, **Sethuraman K**, **Thom SR.** Microparticle formation by platelets exposed to high gas pressures – an oxidative stress response. *Free Radic Biol Med* 101: 154–162, 2016. doi:10.1016/j.freeradbiomed.2016.10.010.
47. **Moroianu J**, **Fett JW**, **Riordan JF**, **Vallee BL.** Actin is a surface component of calf pulmonary artery endothelial cells in culture. *Proc Natl Acad Sci USA* 90: 3815–3819, 1993. doi:10.1073/pnas.90.9.3815.
48. **Cypryk W**, **Nyman TA**, **Matikainen S.** From inflammasome to exosome-does extracellular vesicle secretion constitute an inflammasome-dependent immune response? *Front Immunol* 9: 2188, 2018. doi:10.3389/fimmu.2018.02188.
49. **Allen PG**, **Janmey PA.** Gelsolin displaces phalloidin from actin filaments. *J Biol Chem* 269: 32916–32923, 1994.
50. **Kinosian HJ**, **Selden LA**, **Estes JE**, **Gershman LC.** Kinetics of gelsolin interaction with phalloidin-stabilized F-actin. Rate constants for binding and severing. *Biochemistry* 35: 16550–16556, 1996. doi:10.1021/bi961891j.
51. **Lind SE**, **Smith DB**, **Janmey PA**, **Stossel TP.** Depression of gelsolin levels and detection of gelsolin-actin complexes in plasma of patients with acute lung injury. *Am Rev Respir Dis* 138: 429–434, 1988. doi:10.1164/ajrccm/138.2.429.
52. **Dudani AK**, **Ganz PR.** Endothelial cell surface actin serves as a binding site for plasminogen, tissue plasminogen activator and lipoprotein(a). *Br J Haematol* 95: 168–178, 1996.
53. **Fu L**, **Han L**, **Xie C**, **Li W**, **Lin L**, **Pan S**, **Zhou Y**, **Zhi L**, **Jin M**, **Zhang A.** Identification of extracellular actin as a ligand for triggering receptor expressed on myeloid cells-1 signaling. *Front Immunol* 8: 917, 2017.
54. **Miles LA**, **Andronicos NM**, **Baik N**, **Parmer RJ.** Cell-surface actin binds plasminogen and modulates neurotransmitter release from catecholaminergic cells. *J Neurosci* 26: 13017–13024, 2006. doi:10.1523/JNEUROSCI.2070-06.2006.
55. **Pardridge WM**, **Nowlin DM**, **Choi TB**, **Yang J**, **Calaycay J**, **Shively JE.** rain capillary 46,000 dalton protein is cytoplasmic actin and is localized to endothelial plasma membrane. *J Cereb Blood Flow Metab* 9: 675–680, 1989. doi:10.1038/jcbfm.1989.95.
56. **Por SB**, **Cooley MA**, **Breit SN**, **Penny R**, **French PW.** Antibodies to tubulin and actin bind to the surface of a human monocytic cell line, U937. *J Histochem Cytochem* 39: 981–985, 1991. doi:10.1177/39.7.1865114.
57. **Smalheiser NR.** Proteins in unexpected locations. *Mol Biol Cell* 7: 1003–1014, 1996. doi:10.1091/mbc.7.7.1003.
58. **Rothmeier AS**, **Marchese P**, **Petrich BG**, **Furlan-Freguia C**, **Ginsberg MH**, **Ruggeri ZM**, **Ruf W.** Caspase-1–mediated pathway promotes generation of thromboinflammatory microparticles. *J Clin Invest* 125: 1471–1484, 2015. doi:10.1172/JCI79329.
59. **Bohgaki M**, **Matsumoto M**, **Atsumi T**, **Kondo T**, **Yasuda S**, **Horita T**, **Nakayama KI**, **Okumura F**, **Hatakeyama S**, **Koike T.** Plasma gelsolin fascilitates interaction between B2 glycoprotein I and A5B1 integrin. *J Cell Mol Med* 15: 141–151, 2011. doi:10.1111/j.1582-4934.2009.00940.x.
60. **Giancotti FG**, **Comoglio PM**, **Tarone G.** Fibronectin-plasma membrane interaction in the adhesion of hemopoietic cells. *J Cell Biol* 103: 429–437, 1986. doi:10.1083/jcb.103.2.429.